A Novel PCF SPR Biosensor Using TiO_2 and Gold Coating for Carcinoma Cell Detection

Gollapalli Venkata Vinod , Venkatrao Palacharla , Haraprasad Mondal , Mohammad Soroosh , Mohammad Javad Maleki * , Sandip Swarnakar *

Posted Date: 26 November 2025

doi: 10.20944/preprints202511.2048.v1

Keywords: photonic crystal fiber; surface plasmon resonance; refractive index; confinement loss; wavelength sensitivity; carcinoma cell

Article

A Novel PCF SPR Biosensor Using TiO_2 and Gold Coating for Carcinoma Cell Detection

Gollapalli Venkata Vinod [1], Venkatrao Palacharla [1], Haraprasad Mondal [2], Mohammad Soroosh [3], Mohammad Javad Maleki [3,*] and Sandip Swarnakar [4,*]

[1] Department of Electronics and Communication Engineering, Godavari Global University, Rajahmundry, Andhra Pradesh 533296, India

[2] Department of Electronics and Communication Engineering, Dibrugarh University, Assam - 786004, India

[3] Department of Electrical Engineering, Shahid Chamran University of Ahvaz, Ahvaz, Iran

[4] Department of Electronics and Communication Engineering, Koneru Lakshmaiah Education Foundation, Vaddeswaram, Guntur-522302, Andhra Pradesh, India

* Correspondence: sswarnakar@kluniversity.in (S.S.); mj.maleki@scu.ac.ir (M.J.M.)

Abstract

A responsive dual-core surface plasmon resonance-based photonic crystal fiber DCSPRPCF biosensor has been present in this study, which has been designed for the early and true detection of carcinoma. It is capable of identifying different types of carcinoma cells such as MDAnderson - Metastatic Breast –231(MDA-MB-231), Michigan Cancer Founda-tion-7(MCF-7), Pheochromocytoma (PC12), and Jurkat Cells. It incorporates a titanium dioxide intermediate layer, thereby improving the joining between the silica fiber and the Au layer at the surface of the plasmonic material, resulting in excellent performance. Carcinoma will be detected by calculating the variation in resonance frequency due to the distinction in ReI among the nutritious and Carcinogenic cells by using the Frequency Investigation method. For MDA-MB-231 cells, the sensor achieves peak responsiveness of 16428.54 nm/RIU when the refractive index changes by 0.014. In addition, more Figure of Merit, with a peak utility of 74.29 RIU^{-1} for PC12 cell detection, guarantees the reliability and accuracy of this sensor.

Keywords: photonic crystal fiber; surface plasmon resonance; refractive index; confinement loss; wavelength sensitivity; carcinoma cell

1. Introduction

Carcinoma is complicated disease characterized by uncontrolled multiplication of atypical cells, which attacks different anatomic sites such as the liver, breast, rectum, lung, stomach, and blood, to which genetic, environmental, infectious, and lifestyle factors are responsible. Physical examination, imaging tests, and pathology analysis are some of the traditional diagnostic techniques that play an important role in early diagnosis[1]. However, Biosensors, especially with the advent of highly sensitive PCF-based SPR sensors [2], will offer promising alternatives. PCFs have a microstructure architecture, single-mode propagation, and optimized dispersion [3]. Their improved light confinement and interaction make them highly sensitive to the refractive index variation of the analyte material involved in carcinoma detection [4,5]. The guiding principle behind SPR is through guided evanescent fields that excite surface plasmon on the metallic surface [6]. Among the plasmonic materials, including aluminum, copper, silver, and gold, gold is preferred because it is very stable and gives strong resonance shifts [7]. Different geometries-V, Bowl, D, Spiral, and dual-core polished configurations of PCF SPR sensors have been designed to optimize spectral response sensitivity [8]. These have shown remarkable progress, and some of them are Titanium Nitride (TiN) coated sensor, which presents 10,000 nm/RIU; twin core PCFs, which shows 8571.43 nm/RIU; and graphene-based photonic crystal sensor, offering 2400.08nm/RIU [9]. Furthermore, new geometries

 doi:10.20944/preprints202511.2048.v1

like hexagon-shaped spiral PCFs and V-shaped Zirconium nitrate (Zr(NO3)4) coated PCFs have shown better performance regarding the detection of breast, cervical, and basal carcinoma [10]. TiO2 and Au coating in biosensors enhances the wavelength sensitivity, sweeping from 5500-10714.28 nm/RIU, further strengthening their potential in distinguishing between Carcinogenic cells from nutritious ones [11,12]. Though SPR-PCF sensors face challenges related to plasmonic layer fabrication, they remain highly sensitive, accurate diagnostic techniques, which are poised to transform biomedical sensing and disease-screening technologies [13].

The sensitivity of PCFSPR to slight modifications in sample refractive index (ReI) is high, and their ability to perceive effectualness can be crucially influenced from outside sources [14]. These sensors can be measuring parameters like refractive index, Deoxyribonucleic acid(DNA), and glucose levels [15]. PCFSPR is highly effectual for biosensing and medical diagnostics, offering fast and accurate biomolecule detection [16].These devices harness a guided evanescent fieldleaking from the fiber core into plasmonic-coated channels to excite surface plasmons at the contact surface between dielectric and metal [17]. This approach enables high-sensitivity detection of uncharacterized substances[18]. An Au-plated ring geometry-based high-sensitivity PCF-SPR biosensor was designed and examines using the finite element method, which could effectively detect carcinoma cells across refractive indices extended from 1.360 to 1.401. [19].Gold is selected as the plasmonic metal due to its environmental friendliness, corrosion resistance, and biocompatibility [20].While TiO_2 serves as an adhesion-promoting layer between the fiber and the gold [21]. Light hits a metal surface at a precise angle to cause surface plasmons that respond to changes in ReI near by. As biomolecules attach to the surface, this resonance shifts producing detectable imbalance in the magnitude and direction of the reflections that correspond directly to the biomolecule concentration[22].PCF is grouped into two types, depending on light guiding mechanism of fiber index guiding(IG) PCF and photonic band gap PCF[23]. IGPCF has a high-index solid core bounded by a low-index fine pattern overlay, guiding light through total internal reflection[24].Each type of carcinoma cell produces a characteristic resonance peak, much like a molecular fingerprint allowing precise identification based on the shape and shift of the resonance signal[25].The air holes(AH) patterned throughout the PCF's overlay enable the fiber to confine biological or chemical samples whether gas or liquid within its core or external and internal sensing channels[26].

The current work develops a biosensor that can identify biomolecules with wavelengths range 700nm to 1200nm. Section 2 provides and specifies the suggested design while Section 3 mathematical calculations. Section 4 &5 provides results and comparisons of past work respectively. Section6 provides conclusion of the given work.

2. Structural Modeling and Theoretical Analysis

The proposed Au-TiO_2 coated PCFSPR refractometric sensor is fabricated with a multi-layered cylindrical structure and Mesh model, as shown in Figure 1, optimized for the detection of several Carcinogenic cells. Figure 1a illustrates the geometry of DCSPRPCF, consisting four different layers from the outermost to the innermost region. The outermost perfectly matched layer (PML), possessing broadness of 0.012 nm, helps to reduce unwanted reflections and scattering losses and improve the accuracy of sensing. Under this, the analyte Layer, 1.3 μm thick, functions as the active sensing region where the biological sample either normal or Carcinogen interacts with the optical field to find refractive index with sweep of 1.376 to 1.401, corresponding to variable cell types.

 doi:10.20944/preprints202511.2048.v1

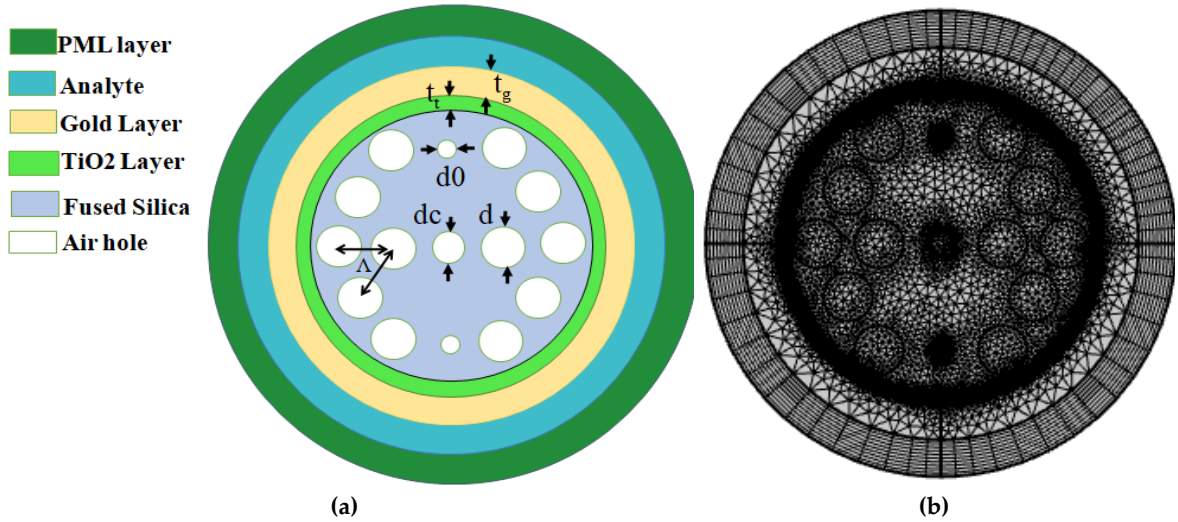

Figure 1. Proposed DCSPRPCF (a) Cross-sectional view of Geometry (b) Physics Controlled Mesh.

The next internal layer is the Au Layer, with a broadness of 0.045 μm, which acts as the plasmonic material due to its outstanding electrical conductivity and chemical balance. Surface Plasmon Polaritons (SPPs) are stimulated at the junction of this metal cover, entitle sensitive refractive index detection. A thin TiO_2 Layer with broadness of 0.038 μm is embedded beneath the gold film. This layer enhances optical characteristics and acts as an adhesive interface to boost the coupling effectiveness among core and SPP mode. The suggested biosensor contains AH well-ordered in a hexagonally packed triangular arrangement and a uniform pitch (Λ) of 2 μm. These AH inserted in quartz glass, enable efficient long-distance light transmission and serve various functional roles. Core is formed by omitting AH, where light propagation occurs. Two minor AHs measuring d_0 = 0.3μm are positioned vertically to reduce efficient coupling of guided modes. To enhance the transient electromagnetic field within the core, One AH is located at center with a diameter d_c = 0.9μm. Larger overlay AH with a diameter d = 1.6μm surround the core, helping to confine the optical mode within the core region, which allow enough light to improve sensor performance. Figure 1b demonstrates the mesh analysis for the suggested biosensor, is set to element size normal, total number of vertex elements 156, 5078 total number of boundary elements.

Figure 2 shows the experimental setup consists of a wideband optical source that injects light all over a single-mode optical fiber into PCFSPR sensor, which features micro structured air hole overlay and a TiO_2-Au plasmonic coating interfacing with the analyte. After exiting the sensor through a secondary single-mode fiber, the light enters an optical spectrum analyzer, which captures its spectral profile and displays resonance dips that indicate specific characteristics of the analyte. Finally, the connected computer processes and visualizes the acquired data for further analysis where separate resonance frequency shifts indicate variations in ReI associated with different carcinoma-cell types. Overall, the connected computer processes and visualizes the acquired data for analysis and interpretation.

 doi:10.20944/preprints202511.2048.v1

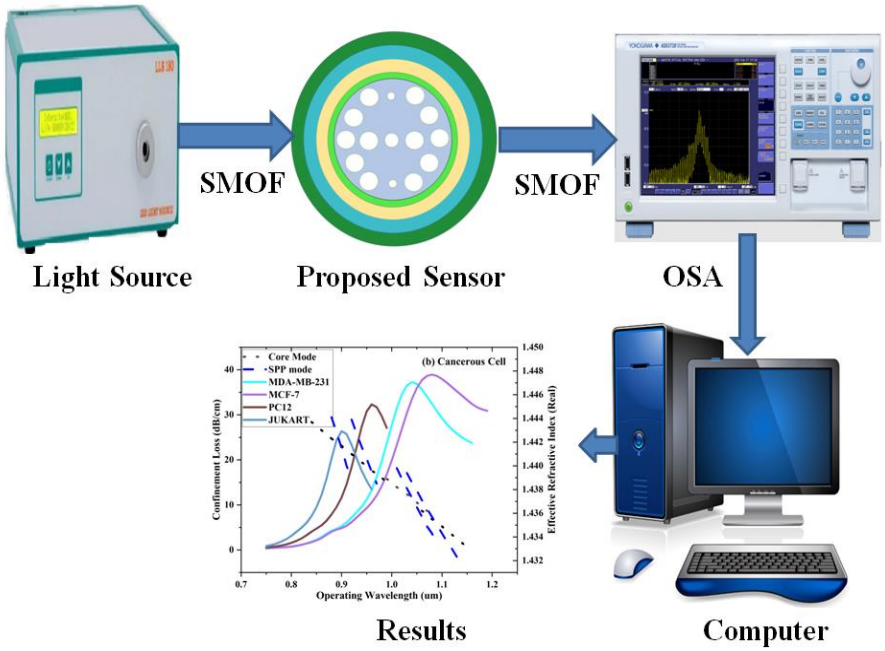

Figure 2. Experimental configuration of DCSPRPCF biosensor.

3. Mathematical Calculations

In the proposed sensor, quartz glass is used for the overlay and PML and the Sellmeier equation (1) is used to find out its ReI.

$$n^2_{silica}(\lambda) = 1 + \frac{0.6961663\,\lambda^2}{\lambda^2 - (0.0684043)^2} + \frac{0.4079426\,\lambda^2}{\lambda^2 - (0.1162414)^2} + \frac{0.8974794\,\lambda^2}{\lambda^2 - (9.896161)^2} \quad (1)$$

n_{silica} is the ReI of quartz glass and operating wazvelength denoted by λ in micrometers (μm).

To establish a good channel enabling light to move from core to outer metal surface and to provide the plasmonic resonance effect, aurum (Au) is used. Drude-Lorenz formula shown in equation (2) is used to compute the ReI of gold.

$$\varepsilon_{Au}(\omega) = \varepsilon_\infty - \frac{\omega_D^2}{\omega(\omega + i\,\gamma_D)} - \frac{\Delta\epsilon.\,\Omega_L^2}{(\omega^2 - \Omega_L^2) - i\,\Gamma_L\omega} \quad (2)$$

$\varepsilon_{Au}(\omega)$ is permittivity of Au, Ω_L is oscillator -strength, $\Delta\epsilon$ is weighted coefficient, ω_D is plasmon-frequency, ε_∞ is high-frequency dielectric constant,damping frequency γ_D, Γ_L is Lorentz Oscillator's frequency bandwidth along with their values are given in Table 1.

Table 1. Tabulated Drude and Lorentz Model Coefficients.

ε_∞	$\frac{\gamma_D}{2\pi}$ (THz)	$\frac{\Gamma_L}{2\pi}$ (THz)	$\frac{\omega_D}{2\pi}$ (THz)	$\frac{\Omega_L}{2\pi}$ (THz)	$\Delta\epsilon$
5.9673	15.92	104.86	2113.6	650.07	1.09

TiO_2 is used to improve the energy transfer efficiency between thequartz glass and the plasmonic layer.The following empirical relationship is used to calculate RI of TiO_2, represented as n_{TiO2} in equation (3).

$$n^2_{TiO2} = 5.913 + \frac{2.441 \times 10^7}{(\lambda^2 - 0.803 \times 10^7)} \quad (3)$$

n_{TiO2} is TiO_2 refractive index, operating wavelength denoted by λ, expressed in Angstrom units.

 doi:10.20944/preprints202511.2048.v1

The core-mode CL is an essential for PCF based SPR sensors and can be derived using equation (4).

$$\alpha_{CL}\left(\frac{dB}{cm}\right) = \frac{20}{\ln 10}\frac{2\pi}{\lambda}\mathrm{I_m(neff)} = 8.686\mathrm{k_0 I_m(neff)} \times 10^4 \quad (4)$$

k_0=2π/λ is a constant, wavelength denoted by λ measured in micrometers (μm) and $\mathrm{I_m}$is the unreal part of the ReI.

Wavelength sensitivity, which mentions to adopt in resonance frequency as a function of varying RI, is used to describe the efficiency of the sensor. This can be represented equation(5).

$$S_\lambda\left(\frac{nm}{RIU}\right) = \frac{\Delta\lambda_{\mathrm{peak}}}{\Delta \mathrm{n_a}} \quad (5)$$

$\Delta\lambda_{peak}$ is a Resonant frequency shift of infected and nutritious cells, Δn_a is the difference between the ReI of malignant and nutritious cells.

Resolution is also an important metric, apart from the amplitude sensitivity. With high sensor resolution, it is also possible to recognize even the smallest differences in ReI between nutritious and carcinoma affected cells. Resolution is calculated using equation (6).

$$\text{Res (RIU)} = \Delta \mathrm{n_a} \times \frac{\Delta\lambda_{\mathrm{min}}}{\Delta\lambda_{\mathrm{peak}}} \quad (6)$$

$\Delta \mathrm{n_a}$ is the difference between the RI of the diseased carcinoma cell and normal cell, $\Delta\lambda_{\mathrm{min}}$ is minimum frequency, and this is set to $0.1\mathrm{nm}$ as a constant value. Sensing performance can also be evaluated using FoM metric; equation (7) is used to calculate the FoM.

$$\text{Figure of Merit (RIU}^{-1}) = \frac{S_\lambda}{\mathrm{FWHM}}\ \mathrm{RIU}^{-1} \quad (7)$$

S_λ is Wavelength sensitivity of a specific carcinoma cell.

4. Simulation Results and Analysis

Light propagation through the core of a PCF cause an evanescent field that influence with transition region between metal and dielectric, enabling the induction of surface plasmon oscillations. This interaction serves as the foundation for SPR sensing, which is more sensitive to converts in the surrounding ReI an essential feature for bio-sensing. This study emphasizes the x-polarized mode, which shows more loss than the y-polarized mode, indicating stronger light-matter interaction and more sensitivity. Figure 3 shows the energy density layout of the core position, SPP position, demonstrating the energy transfer across modes in their coupled position for the MCF-7 cell, which includes both normal and Carcinogenic cells.

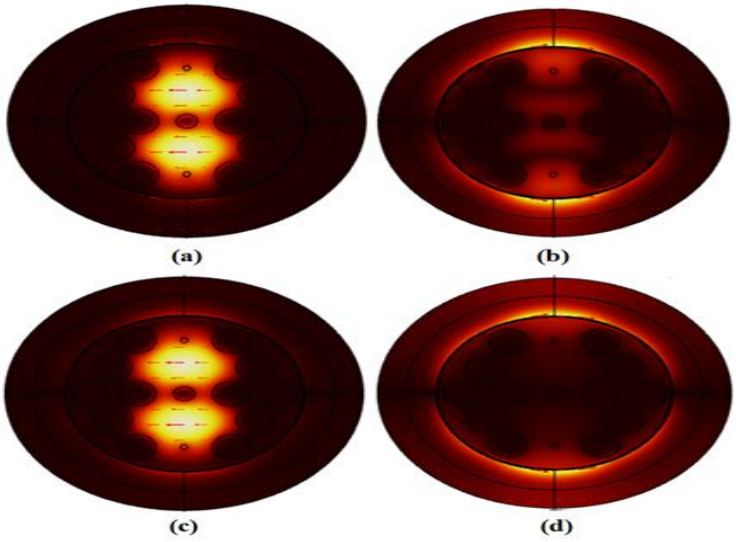

FigureF3. X-Polarized Electric field distribution (2D view), for Breast Carcinoma Type-2 cell (a) Core (normal), (b) SPP(normal), (c) Core(infected), (d) SPP(infected).

 doi:10.20944/preprints202511.2048.v1

Figure 4a,b gives the dissimilarity of **confinement loss (CL)**and **effectual refractive index (ERI)**for both the SPP and core modes as a Frequency. The analysis is for both nutritious and Carcinogenic cells similar with **breast carcinoma type-1and type-2, adrenal gland carcinoma,** and **blood carcinoma.** For each type of cell**,** the **joining point** between the ERI curves of the core and SPP positions trace the **resonance frequency,** where a clear**peak in CL** is detected**.** This peak indicates the phase synchronization condition, where the actual areas of the effectual ReI of SPP and core position are equal, for identification of Carcinogenic cells.

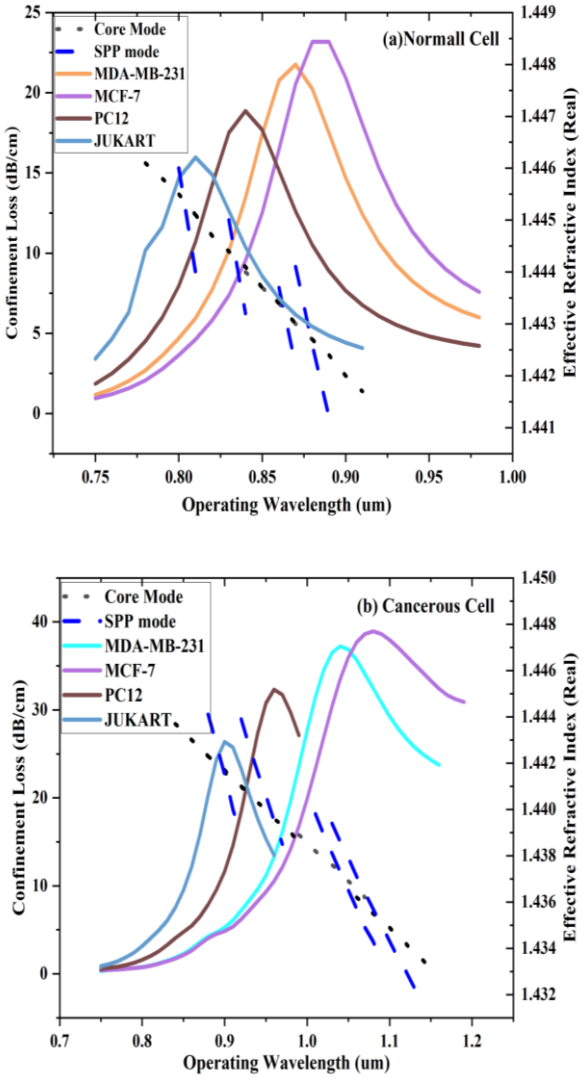

Figure 4. Effective ReI and Loss variance with operating wavelength for MDAMB-231, MCF-7, Jurkat and PC12. (a) Non-Malignant Cell (b) Malignant Cell.

Figure 5 shows the scattering spectra for Breast Carcinoma Type-1,Breast Carcinoma Type-2, Adrenal Glands and Blood Carcinoma cells. For Breast Carcinoma Type-1, resonance peaks are located at 0.87μm (normal) and 1.1μm (Carcinogenic), corresponding to a 230nm shift. In such a situation of Breast Carcinoma Type-2 cells, peaks appear at 0.88μm (normal) and 1.1μm (Carcinogenic), showing a 220 nm shift. In the case of Adrenal Glands cells, peaks appear at 0.84μm (normal) and0.97μm (Carcinogenic), showing a 130nm shift. In the case of Blood Carcinoma cells, peaks appear at 0.81μm (normal) and 0.91 μm (Carcinogenic), showing a 100 nm shift.

 doi:10.20944/preprints202511.2048.v1

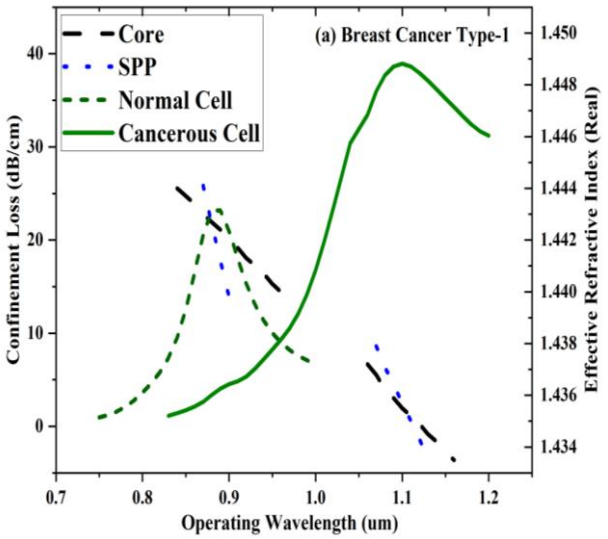

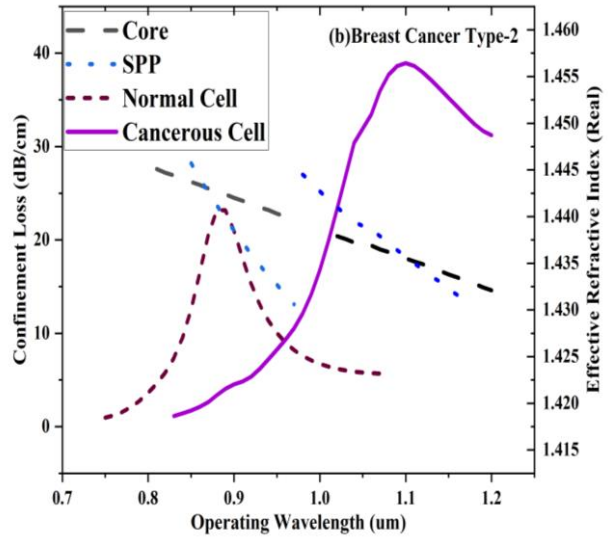

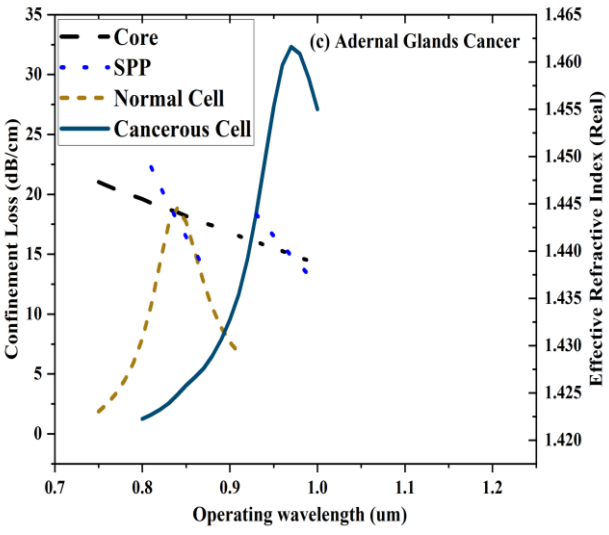

 doi:10.20944/preprints202511.2048.v1

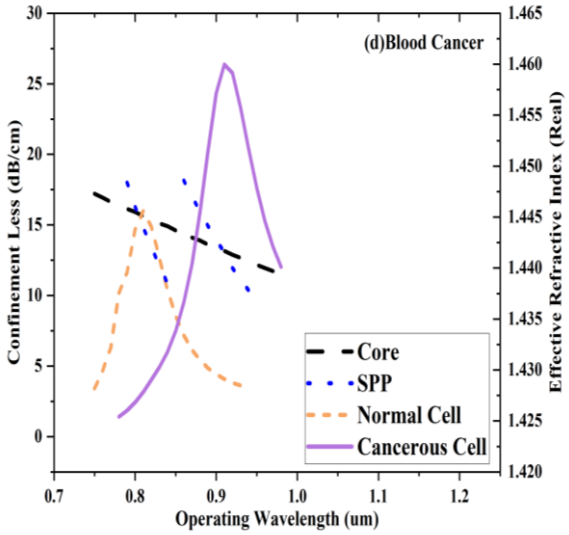

Figure 5. Variance of CL and actual part of effectualReI with operating wavelength for (a) MDAMB-231 (b) MCF-7 (c) PC12 and (d)Jurkat for the proposed PCF.

5. Evaluation of Proposed Sensor Against Previously Reported Works

Plasmonic biosensors using Photonic Crystal Fibers (PCFs) are emerging as effective tools for early cancer detection because of their strong light confinement and surface plasmon resonance effects. Several PCF structures Dual-core, Hexagonal, Spiral, D-type, and slotted have been designed and applied for detecting cancers such as Jurkat, PC12, MDA-MB-231, and MCF-7. Gold is the most widely utilize plasmonic layer, while composite coatings with TiO_2, Graphene, MXene, and Black Phosphorus further boost sensitivity, stability, and biocompatibility. Among the reported models, the dual-core hexagonal lattice PCF achieves maximum wavelength sensitivity (16,428 nm/RIU), whereas the dual-core dual-polished PCF demonstrates the highest figure of merit (125) with excellent resolution (~1.4×10^{-6} RIU).

Table 2. Analysis of Proposed DC-SPR-PCF Biosensor Compared to Previous Models.

Carcinoma Cell Type	Geometric Structure	Plasmonic Material	WS (nm/RIU)	AS (RIU^{-1})	FoM	Resolution (RIU)	Reference
BLC	Dual-core dual-polished PCF	Au	5714	-203	78	1.8×10^{-5}	[21]
AeGC			6429	-259	60	1.6×10^{-5}	
BCT1			7143	-270	125	1.4×10^{-6}	
BCT2			7143	-249	100	1.4×10^{-6}	
BLC	Dual-core oblong PCF	Au, TiO_2	6,071	-897.37	117	1.65×10^{-5}	[18]
AeGC			7,500	-1195.73	119.6	1.33×10^{-5}	
BCT1			9,643	-1251.18	79.9	1.04×10^{-5}	
BCT2			11,429	-1115.12	65.08	8.75×10^{-6}	
BLC	Twin-Core PCF with circular	Au, TiO_2	3571	-2172.31	2.8	2.80×10^{-5}	[4]
AeGC			3571	-2537.37	2.8	2.80×10^{-5}	
BCT1			4285	-2193.76	2.33	2.33×10^{-5}	
BCT2			4285	-1813.13	2.33	$2.33 \times 10^{-}$	

 doi:10.20944/preprints202511.2048.v1

BLC	Dual-core PCF with bilateral surface	Au	4285.72	-457.087	n.r	2.33×10^{-5}	[3]
AeGC			4285.72	-750.443	n.r	2.33×10^{-5}	
BCT1			5714.28	-735.512	n.r	1.75×10^{-5}	
BCT2			5714.28	-899.248	n.r	1.75×10^{-5}	
BLC	Spiral-Shaped PCF	Au	n.r	-165.9	n.r	1.4×10^{-4}	[22]
AeGC			n.r	-245.5	n.r	1.4×10^{-4}	
BCT1			n.r	-289	n.r	2.33×10^{-4}	
BCT2			n.r	-154.5	n.r	2.33×10^{-4}	
BCT1	Hexagonal lattice PCF	Au,TiO_2	9428.57	-1441	n.r	1.06×10^{-5}	[24]
BCT2			10714.28	-1411	n.r	0.93×10^{-5}	
AeGC			7571.43	-1452	n.r	1.32×10^{-5}	
BLC			6000	-1599	n.r	1.67×10^{-5}	
BLC	Hexagonal PCF	Au	4642.86	-401	n.r	2.2×10^{-5}	[30]
AeGC			5500	-399	n.r	1.8×10^{-5}	
BCT1			6428.57	-324	n.r	1.6×10^{-5}	
BCT2			7142.86	-305	n.r	1.4×10^{-5}	
BLC	D-Type, hexagonalPCF	Au/Graphene/Ti_3C_2Tx-MXene	5714	303.56	n.r	2.2×10^{-5}	[31]
AeGC			7143	346.03	n.r	1.8×10^{-5}	
BCT1			8571	330.05	n.r	1.6×10^{-5}	
BCT2			9286	309.53	n.r	1.4×10^{-5}	
BLC	Slotted D-shaped PCF	Au, TiO_2,Black Phosphorus	6071	n.r	n.r	n.r	[32]
AeGC			9286	n.r	n.r	n.r	
BCT1			11,429	n.r	n.r	n.r	
BCT2			10,714	n.r	n.r	n.r	
BLC	Dual-core dual-polished PCF-SPR	Au	5714	-203	78	1.8×10^{-5}	[33]
AeGC			6429	-259	60	1.6×10^{-5}	
BCT1			7143	-270	125	1.4×10^{-5}	
BCT2			7143	-249	100	1.4×10^{-5}	
BCT1	Dual-core PCF with Hexagonal lattice	Au,TiO_2	16428.54	n.r	68.42	6.09×10^{-6}	Proposed Model
BCT2			15714.23	n.r	65.47	6.36×10^{-6}	
AeGC			9285.71	n.r	74.29	1.08×10^{-5}	
BLC			7142.35	n.r	62.11	1.4×10^{-5}	

n.r: not required

6. Conclusion

The **dual core surface plasmon resonance based photonic crystal fiber (DCSPRPCF) biosensor** demonstrates **extraordinary performance** in early carcinoma cell detection, specifically targeting **Jurkat, MDA-MB-231, PC12, and MCF-7 cells**. It has high sensitivity to refractive index changes. wavelength sensitivity varies from 7142.85nm/RIU up to 16428.57nm/RIU. Its high precision is

 doi:10.20944/preprints202511.2048.v1

reflected in the refractive index resolution that ranges from 1.08× 10-6 RIU and 6.36× 10-6 RIU. It provides the highest Figure of Merit in Adrenal glands carcinoma cell detection and further evidences its precision and reliability in carcinoma diagnostics. The **DCSPRPCF biosensor** emerges as a **highly efficient and precise solution** for early-stage carcinoma diagnostics, offering an **advanced, sensitive, and dependable platform** for accurately detecting malignant cells.

Declarations

Ethical Approval: Not required.

Acknowledgements: The authors declare that no funds, grants, or other support were received during the preparation of this manuscript.

Consent to participate: For this type of study formal consent is not required.

Consent for publication: Not applicable.

Funding: No funding is received for this manuscript.

Conflicts of interest/Competing interests: The authors declare that they have no known competing financial interests or personal relationships that could have appeared to influence the work reported in this paper.

Data availability: We can provide the data as per request.

Authors' contributions: Gollapalli Venkata Vinod: Investigation; Formal analysis, Writing - original draft, Methodology. Venkatrao Palacharla: Investigation; Formal analysis; Supervision. Haraprasad Mondal: Formal analysis, Methodology; Data Curation. Mohammad Soroosh: Formal analysis, Methodology; Software. Mohammad Javad Maleki: Prepared figures, Methodology. Sandip Swarnakar: Conceptualization; Validation; Writing - review & editing; Supervision.

 doi:10.20944/preprints202511.2048.v1

Abbreviations

Table 3. List of Abbreviations.

S.No.	Acronym	Full Form
1	AeGC	Adrenal Gland Cancer
2	AH	**Air Holes**
3	Au	Gold
4	BCT1	Breast Cancer Type-1
5	BCT2	Breast Cancer Type-2
6	BLC	Blood Cancer
7	CL	**Confinement Loss**
8	DC-SPR-PCF	Dual Core-Surface Plasmon Resonance-Photonic Crystal Fiber
9	DNA	**Deoxyribonucleic acid**
10	FoM	**Figure of Merit**
11	IG	**Index Guiding**
12	PCF	**Photonic Crystal Fiber**
13	PC12	Pheochromocytoma
14	PML	Perfectly Matched Layer
15	ReI	**Refractive Index**
16	SPP	**Surface Plasmon Polarization**
17	SPR	**Surface Plasmon Resonance**
18	MDA-MB-231	M D **Anderson - Metastatic Breast** – 231
19	MCF-7	**Michigan Cancer Foundation-7**
20	TiO_2	Titanium Dioxide
21	TiN	Titanium Nitride
22	$Zr(NO_3)_4$	**Zirconium nitrate**

References

1. Rachana, M.; Charles, I.; Swarnakar, S.; Krishna, S.V.; Kumar, S. Recent advances in photonic crystal fiber-based sensors for biomedical applications. *Opt. Fiber Technol.* 2022, 74, 1–12. https://doi.org/10.1016/j.yofte.2022.103085

 doi:10.20944/preprints202511.2048.v1

2. Hasan, M.R.; Akter, S.; Rifat, A.A.; Rana, S.; Ali, S. A highly sensitive gold-coated photonic crystal fiber biosensor based on surface plasmon resonance. *Photon.* 2017, 4, 1–11. https://doi.org/10.3390/photonics4010018
3. Nagavel, B.; Dagar, H.; Krishnan, P. High-Performance Dual-Core Bilateral Surface Optimized PCF SPR Biosensor for Early Detection of Six Distinct Cancer Cells. *Plasmon.* 2025, 20, 4799–4809. https://doi.org/10.1007/s11468-024-02661-2
4. Ibrahimi, K.M.; Kumar, R.; Pakhira, W. Enhance the Design and Performance Analysis of a Highly Sensitive Twin-Core PCF SPR Biosensor with Gold Plating for the Early Detection of Cancer Cells. *Plasmon.* 2023, 18, 995–1006.
5. https://doi.org/10.1007/s11468-023-01825-w
6. Swarnakar, S.; Anguluri, S.P.K.; Alluru, S.; Kumar, S. A novel structure of all-optical optimised NAND, NOR and XNOR logic gates employing a Y-shaped plasmonic waveguide. *Opt. Quant. Electron.* 2022, 54, 1–17.
7. https://doi.org/10.1007/s11082-022-03911-5
8. Akter, S.; Abdullah, H. Design and Investigation of High-Sensitivity PCF SPR Biosensor for Various Cancer Cells Detection Using a Gold-Coated Circular-Shaped Structure. *Plasmon.* 2025, 20, 5303–5313.
9. https://doi.org/10.1007/s11468-024-02727-1
10. Singh, S.; Kumar, R.; Chaudhary, B.; Bhardwaj, P.; Upaddhyay, V.K.; Upadhyay, A.; Daher, M.G. Gold Immobilized SPR-Enhanced PCF Biosensor for Detection of Cancer Cells: A Numerical Simulation. *Plasmon.* 2025, 20, 3535–3544.
11. https://doi.org/10.1007/s11468-024-02578-w
12. Mahbub, S.M.; Nafiz, A.A.M.; Protiva, A.A.; Tamim, M.; Rahad, R. Ultra-short pulse: A comprehensive way of sensing pure solvents through hollow core photonic crystal fiber sensor. *Opt. Mater.* 2024, 156, 116028.
13. https://doi.org/10.1016/j.optmat.2024.116028
14. Singh, S.; Upadhyay, A.; Chaudhary, B.; Sirohi, K.; Kumar, S. Enhanced Cu-Ni-TiO-BP plasmonic biosensor for highly sensitive biomolecule detection and SARS-CoV-2 diagnosis. *IEEE Sens. J.* 2023, 24, 254–261.
15. https://doi.org/10.1109/JSEN.2023.3334104
16. Malek, C.; Al-Dossari, M.; Awasthi, S.K.; Matar, Z.S.; El-Gawaad, N.S.A.; Sabra, W.; Aly, A.H. Employing the defective photonic crystal composed of nanocomposite superconducting material in detection of cancerous brain tumors. *Crystals* 2022, 12, 1–21. https://doi.org/10.3390/cryst12040540
17. Mollah, M.A.; Yousufali, M.; Ankan, I.M.; Rahman, M.M.; Sarker, H.; Chakrabarti, K. Twin core photonic crystal fiber refractive index sensor for early detection of blood cancer. *Sens. Bio-Sens. Res.* 2020, 29, 1–6.
18. https://doi.org/10.1016/j.sbsr.2020.100344
19. Mishra, G.P.; Kumar, D.; Chaudhary, V.S.; Sharma, S. Terahertz refractive index sensor with high sensitivity based on two-core photonic crystal fiber. *Microw. Opt. Technol. Lett.* 2021, 63, 24–31. https://doi.org/10.1002/mop.32573
20. Azab, M.Y.; Hameed, M.F.O.; Nasr, A.M.; Obayya, S.S.A. Label-free detection for DNA hybridization using surface plasmon photonic crystal fiber biosensor. *Opt. Quant. Electron.* 2018, 50, 1–13. https://doi.org/10.1007/s11082-017-1302-2
21. Swarnakar, S.; Anguluri, S.P.K.; Kumar, S. Design and analysis of miniaturized all-optical binary to gray code converter using Y-shaped plasmonic waveguide. *Photon. Netw. Commun.* 2022, 44, 21–29.
22. https://doi.org/10.1007/s11107-022-00976-w
23. Singh, S.; Chaudhary, B.; Upadhyay, A.; Sharma, D.; Ayyanar, N.; Taya, S.A. A review on various sensing prospects of SPR based photonic crystal fibers. *Photon.* 2023, 54, 101119. https://doi.org/10.1016/j.photonics.2023.101119
24. Srivastava, R.; Pal, S.; Prajapati, Y.K. MXene-Assisted D-Shaped Photonic Crystal Fiber Probe with High Sensitivity for Detection of Tuberculosis. *Plasmon.* 2023, 18, 2049–2058. https://doi.org/10.1007/s11468-023-01924-8
25. Akter, S.; Abdullah, H. Design and Investigation of High-Sensitivity PCF SPR Biosensor for Various Cancer Cells Detection Using a Gold-Coated Circular-Shaped Structure. *Plasmon.* 2025, 20, 5303–5313.

 doi:10.20944/preprints202511.2048.v1

26. https://doi.org/10.1007/s11468-024-02727-1
27. Majeed, M.F.; Ahmad, K.A. Design and analysis of a dual-core PCF biosensor based on SPR for cancerous cells detection. *Opt. Quant. Electron.* 2024, 56, 1030. https://doi.org/10.1007/s11082-024-06566-6
28. Amiri, T.; Kadivar, E.; Ghajarpour-Nobandegani, S. Cancer Cell Detection Using a Dual-Core Photonic Crystal Fiber Based on Surface Plasmon Resonance. *Sens. Imaging* 2024, 25, 42. https://doi.org/10.1007/s11220-024-00494-1
29. Mahalaxmi, G.; Tirupal, T.; Shanawaz, S.; Swarnakar, S.; Krishna, S.V. A comparison and survey on brain tumour detection techniques using MRI images. *Curr. Signal Transduct. Ther.* 2023, 18, 14–23.
30. https://doi.org/10.2174/1574362417666220601162839
31. Ayyanar, N.; Raja, G.T.; Sharma, M.; Kumar, D.S. Photonic crystal fiber-based refractive index sensor for early detection of cancer. *IEEE Sens. J.* 2018, 18, 7093–7099. https://doi.org/10.1109/JSEN.2018.2854375
32. Shweta, M.; Saharia, A.; Ismail, Y.; Petruccione, F.; Bourdine, A.V.; Morozov, O.G.; Demidov, V.V.; Yin, J.; Singh, G.; Tiwari, M. Spiral-shaped photonic crystal fiber-based surface plasmon resonance biosensor for cancer cell detection. *Photon.* 2023, 10, 230. https://doi.org/10.3390/photonics10030230
33. Swarnakar, S.; Noonepalle, H.; Raju, K.S.R.; Ramarao, G.; Ramamurthy, N.; Kumar, S. Implementation of all-optical 3-dB and 10-dB directional coupler for switching applications. *Photon. Netw. Commun.* 2023, 45, 107–114.
34. https://doi.org/10.1007/s11107-023-00995-1
35. Chaudhary, V.S.; Kumar, D.; Kumar, S. Au–TiO_2 coated photonic crystal fiber based SPR refractometric sensor for detection of cancerous cells. *IEEE Trans. Nanobiosci.* 2023, 22, 562–569. https://doi.org/10.1109/TNB.2022.3219104
36. Gangwar, R.K.; Singh, V.K. Highly sensitive surface plasmon resonance based D-shaped photonic crystal fiber refractive index sensor. *Plasmon.* 2017, 12, 1367–1372. https://doi.org/10.1007/s11468-016-0395-y
37. Paul, A.K.; Habib, M.S.; Hai, N.H.; Razzak, S.M.A. An air-core photonic crystal fiber based plasmonic sensor for high refractive index sensing. *Opt. Commun.* 2020, 464, 125556. https://doi.org/10.1016/j.optcom.2020.125556
38. Liu, Z.; Liu, X.; Singh, R.; Li, G.; Swarnakar, S.; Zhang, B. Laser-based four-core biosensor with WS_2 thin-film/CeO_2-nanorods/AuNPs immobilization for ascorbic acid detection. *IEEE Sens. J.* 2023, 23, 27215–27223.
39. https://doi.org/10.1109/JSEN.2023.3323392
40. Khetani, A.; Momenpour, A.; Alarcon, E.I.; Anis, H. Hollow core photonic crystal fiber for monitoring leukemia cells using SERS. *Biomed. Opt. Express* 2015, 6, 4599–4609. https://doi.org/10.1364/BOE.6.004599
41. Jahan, N.; Rahman, M.M.; Ahsan, M.; Based, M.A.; Rana, M.M.; Gurusamy, S. Photonic crystal fiber-based biosensor for Pseudomonas bacteria detection. *IEEE Access* 2021, 9, 42206–42215. https://doi.org/10.1109/ACCESS.2021.3063691
42. Yasli, A. Cancer detection with surface plasmon resonance-based photonic crystal fiber biosensor. *Plasmon.* 2021, 16, 1605–1612. https://doi.org/10.1007/s11468-021-01425-6
43. Mao, Y.; Ren, F.; Zhou, D.; Li, Y. Highly sensitive PCF-SPR RI sensor for cancer detection using gold/graphene/Ti_3C_2Tx-MXene hybrid layer. *Plasmon.* 2025, 20, 2279–2290. https://doi.org/10.1007/s11468-024-02467-2
44. Bhuyan, A.; Khamaru, A.; Kumar, A. Black phosphorus-based slotted D-shaped PCF SPR sensor for cancer detection. *Plasmon.* 2025, 20, 5201–5213. https://doi.org/10.1007/s11468-024-02715-5
45. Sardar, M.R.; Faisal, M. Dual-core dual-polished PCF-SPR sensor for cancer cell detection. *IEEE Sens. J.* 2024, 24, 9843–9854. https://doi.org/10.1109/JSEN.2024.3358173